

---

# CHOOSING A SAMPLING FREQUENCY FOR ECG QRS DETECTION USING CONVOLUTIONAL NETWORKS

---

A PREPRINT

**Ahsan Habib**  
School of Information Technology  
Deakin University  
Geelong, Australia 3225  
mahabib@deakin.edu.au

**Chandan Karmakar**  
School of Information Technology  
Deakin University  
Geelong, Australia 3225  
karmakar@deakin.edu.au

**John Yearwood**  
School of Information Technology  
Deakin University  
Geelong, Australia 3225  
john.yearwood@deakin.edu.au

December 30, 2021

## ABSTRACT

Automated QRS detection methods depend on the ECG data which is sampled at a certain frequency, irrespective of filter-based traditional methods or convolutional network (CNN) based deep learning methods. These methods require a selection of the sampling frequency at which they operate in the very first place. While working with data from two different datasets, which are sampled at different frequencies, often, data from both the datasets may need to resample at a common target frequency, which may be the frequency of either of the datasets, or could be a different one. However, choosing data sampled at a certain frequency may have an impact on the model's generalisation capacity, and complexity. There exists some studies that investigate the effects of ECG sample frequencies on traditional filter-based methods, however, an extensive study of the effect of ECG sample frequency on deep learning-based models (convolutional networks), exploring their generalisability and complexity is yet to be explored. This experimental research investigates the impact of six different sample frequencies (50, 100, 250, 500, 1000, and 2000Hz) on four different convolutional network based models' generalisability (subject-wise intra and inter-database validation with three different datasets from PhysioNet bank) and complexity in order to form a basis to decide on an appropriate sample frequency for the QRS detection task for a particular performance requirement. Intra-database tests report an accuracy improvement no more than approximately 0.6% from 100Hz to 250Hz and the shorter interquartile range for those two frequencies for all CNN-based models. The findings reveal that convolutional network-based deep learning models are capable of scoring higher levels of detection accuracies on ECG signals sampled at frequencies as low as 100Hz or 250Hz while maintaining lower model complexity (number of trainable parameters and training time).

**Keywords** Deep learning · Convolutional Neural Network (CNN) · Generalization · ECG · QRS complex · Sampling frequency

## 1 Introduction

Electrocardiogram (ECG) is a non-invasive technique of diagnosing heart conditions. ECG signals consist of a P wave, a QRS complex and a T wave, among which the QRS complex is the most prominent and can easily be detected by a cardiologist. The automated analysis of ECG signals requires these basic ECG waves to be detected and the detection of the QRS complex is often the basis of detection of the other waves [1]. Sampling frequency of an ECG signal may characterise the quality of the signal in terms of the visibility of the basic waves. A poorly chosen sampling frequency may have an impact on the ECG signal quality, as well as, on the performance of the automated ECG signal analysis, specifically, the QRS detection.

The ECG is a non-stationary (varying mean and variance), highly irregular, and heterogeneous time-series data [2]. ECG signals vary continuously over time and reflects the clinical state of the human body. Recording of the ECG

signals generally contains different types of noise (i.e. baseline noise, power-line interference, electrode contact noise) and artifacts (i.e. motion artifacts) [3]. Also, different ECG recordings of the same subject in different recording environments, may produce recordings with different signal characteristics. In addition, ECG recordings of each individual may be deemed to be so unique that it can be used as a bio-metric signature to identify individuals [4]. Due to the non-stationary nature of ECG signals, the inherent subject-wise signal variance and the presence of noise and motion artifacts, the publicly available ECG datasets (i.e. in the PhysioNet data bank) show diverse signal characteristics. For example, the MIT-BIH arrhythmia database [5] consists of a mix of healthy and arrhythmia (with rare but clinically important types) patients, whereas, the INCART database [5] consists of recordings from patients consistent with ischemia, coronary artery disease, conduction abnormalities and arrhythmias (Figure 2 shows three patients with different symptoms), and the QT database [6], on the otherhand, includes ECGs representing a wide variety of QRS and ST-T morphologies and this is a compositional database (combining recordings from other PhysioNet databases). In this study, we aim to analyze the impact of sampling frequency on the performance of QRS detection algorithm.

The impact of sampling frequency on the morphology of ECG signal (healthy individual) is shown in Figure 1. This effect on the pathological or very noisy ECG signals may be worse, which can negatively affect the performance of any QRS detection algorithm. The shape of the QRS complexes may be distorted at lower frequencies and the high frequency signals, which provide finer resolution, however, are likely to contain noise due to the subtle movements. Thus, lower frequency signals may risk losing information that keeps an automated QRS detector from obtaining a desirable performance, and on the otherhand, much higher frequency signals may risk not gaining much information to increase detection performance proportionately and increase the algorithm complexity. The selection of an optimal sample frequency for the QRS detection task is thus desirable to obtain a general detector algorithm.

The selection strategy of the target sample frequency is different in different studies, and includes, choosing the database frequency as the target in a single database-based study [7], choosing one of the database frequencies as the target [8], or choosing an arbitrary target frequency [9]. Automated ECG analysis methods, in the literature, often report their performances against a single target sample frequency. Thus, choosing a single best or optimum target frequency, for a specific task, is an important design decision which may require having a clear understanding of the effects of the sampling frequency on the model's performance.

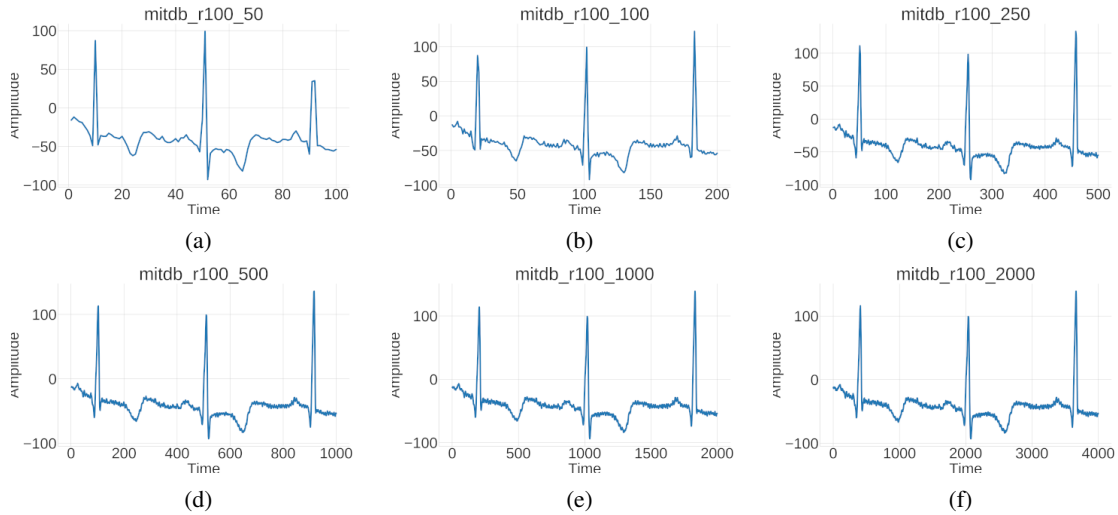


Figure 1: Two seconds ECG signal excerpt of MIT-BIH arrhythmia dataset (record number 100), resampled at all six sample frequencies - (a) 50Hz, (b) 100Hz, (c) 250Hz, (d) 500Hz, (e) 1000Hz, and (f) 2000Hz. The original sample frequency is 360Hz, which was resampled using linear interpolation (using PhysioNet *xform* tool). ECG data at the lowest frequency is less noisy but loses information, on the other hand, higher frequency signals are of finer resolution but comparatively more noisy due to interpolation.

There are different models (or approaches) for the QRS detection task, including, template matching [10], peak-detection-based methods using filters [11], and deep learning (DL) based studies [8, 12]. Different methods' detection performance may vary based on the variation of the sample frequency due to their internal working mechanisms. Filter-based traditional QRS detection methods, for example, use frequency dependent filters (i.e. band-pass filter) which are sample frequency specific and different studies tried to find the sample frequency effects on the model's performance [13, 14, 15] and to minimise them [13, 16]. Deep learning-based methods may also have effects on the

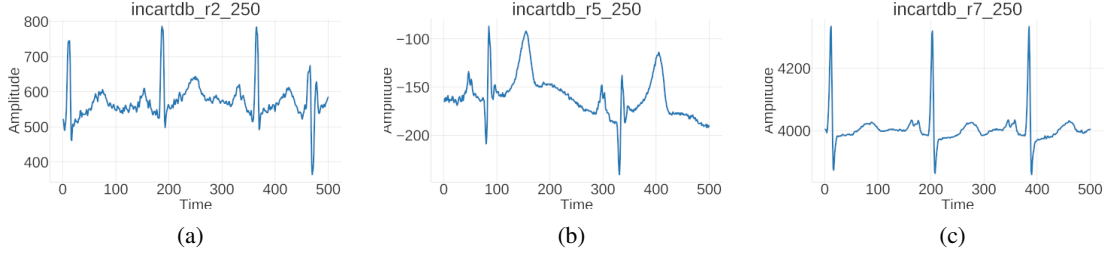


Figure 2: Two seconds ECG signal excerpt of INCART dataset (resampled at 250Hz) of three patients with symptoms of (a) coronary artery disease, arterial hypertension (record number 2), (b) acute MI (record number 5), and (c) transient ischemic attack (record number 7).

variation of the sampling frequency, though not the same way as the filter-based methods mentioned above, which should be investigated.

Deep learning-based approaches for the QRS detection task have been a promising research direction, inspired by success in computer vision. DL-based methods may not be dependent on the data sampled at different frequencies the same way as the filter-based methods would be, however, there are several aspects of the deep learning-based algorithms those may be dependent on the sample frequency of the input signal. It may become intuitive, for the DL-based methods for QRS detection, that due to the loss of information (occurring at the lower sample frequencies), detection performance may go down and on the other hand, due to the cessation of information gain (occured at the higher sample frequencies), the increase of the detection performance may be zero or marginal, but a quantitative analysis seems to be necessary to spot these frequency boundaries and the detection behavior over this range of frequencies. Two features of CNNs: i) having the capability to handle raw input data; and ii) the robustness to noise, make them different from the filter-based methods in detecting QRS complex from ECG signal with varying sampling frequency [17, 18]. As mentioned earlier, the higher sampling frequencies that enable finer resolution input but likely introduce noise, may limit the information gain and thus, may limit the detection performance, but CNNs, equipped with noise tolerance, may show a different performance behavior, which should be properly investigated for the QRS detection.

In our previous work [8], the impact of the diverse ECG datasets was investigated on the generalisation capability of a CNN model for the QRS detection task. The CNN-based model’s generalisability was investigated using subject-wise intra-database and cross-database validation which showed that a single model generalises differently on different databases. Finding a general model for the QRS detection task is desirable, however, not many studies in the literature were found to investigate a single model’s generalisability across multiple ECG databases. While working on three databases, which were sampled at three different frequencies, in that study, the same question of choosing an optimum target sample frequency was encountered and the 360Hz was chosen considering the fact that the MIT-BIH arrhythmia database, which was one of the mostly studied databases, was sampled at that frequency and achieved superior performances in many different studies. However, a thorough study focusing on the effects of the sampling frequency on CNN-based models was missing during our previous work to help us choose an optimum target frequency. In that study, the generalisability of only the proposed CNN model was investigated across multiple databases, however, those findings were not validated across multiple CNN model architectures to affirm the generalisability of DL models.

The current study examines the impact of six different sampling frequencies, between as low as 50Hz and as high as 2000Hz (i.e. 50Hz, 100Hz, 250Hz, 500Hz, 1000Hz, and 2000Hz), on the generalisability of a CNN model. Three publicly available ECG datasets (sampled at three different frequencies), from the PhysioNet databank, were used (i.e. MIT-BIH arrhythmia, INCART, and QT) and subject-wise intra and inter-database validations were carried out for the models generalisability analysis. While the intra-database testing reveals the model’s generalisability for the subjects within a dataset, the inter-database test validates a model’s generalisability beyond the training dataset. Selection of three datasets, in this study, was assumed to ensure the selection of ECG signals with a diverse range of cardiac (patho) physiological characteristics for the QRS detection task. In order to cross validate the findings of the sampling frequency effects on DL models, four different CNN architectures were used (classical convolution-pooling, Fully convolutional networks (FCN) [19, 20], Discriminative filter learning model (DFL) [21], and DenseNet [22]), considering the assumption that these CNN architectures cover a broad range of DL models.

## 2 Methodology

### 2.1 Data resampling

The heart beats at most 220 beats per minutes (which is less than 4Hz), but there are heartbeat signals whose spectrum is up to 25Hz or beyond [13]. For example, a small QRS complex may be 40 ms that corresponds to 25Hz. The Nyquist theorem dictates that the input signal can represent up to half of its sampling frequency [23]. This essentially means that the sampling frequency of the ECG signal should be at least 50Hz to represent a small QRS complex spectrum of 25Hz. To analyse the effect of different sampling frequencies on the CNN model generalisation, six different target sample frequencies were chosen from as low as 50Hz to as high as 2000Hz (i.e., 50, 100, 250, 360, 500, 1000 and 2000Hz). ECG signals below 50Hz may lose information and make the signal unsuitable for the QRS detection task, whereas, a 2000Hz signal represents enough finer resolution, beyond which no additional information may be added to the signal for the specified task. The PhysioNet provided function (*xform*) was found suitable to resample all three datasets (MIT-BIH arrhythmia, INCART, and QT) to six target frequencies, with scaling the annotation data accordingly.

### 2.2 Data segmentation

To localise heartbeats, the ANSI/AAMI EC38 and EC57 standards [24] suggest that an estimated location should be considered accurate if it is within 150 ms from the corresponding annotated location. This implies that a location can be considered as an R-peak if the corresponding annotations point stays around 150 ms of that point, forming a valid window range of 300 ms [12]. ECG recordings from the datasets were segmented with a length of 300 ms equivalent samples following this policy and an overlap of 50% was considered to shift the segment forward. Raw ECG segments were fed without any pre-processing to the CNN model for QRS detection.

### 2.3 CNN Models

To justify the impact of different sampling frequency signals on the CNN models, it was important to use more than one CNN architecture, to understand the general model behavior across different CNN model architectures. Four different CNN model architectures were considered in this study, as below -

- Classical convolution-pooling model (alternate conv-pooling)
- DenseNet
- Fully convolutional network (FCN)
- Discriminative filter learning model (DFL)

Note that there are a plathora of CNN model architectures available in the literature, and considering all of them is impractical, however, some successful model architectures from the computer vision domain may not be suitable for the current context where comparatively shallower CNN models are preferable. For example, an architecture applying residual connection (i.e. ResNet CNN architecture [25]) may generally not be suitable for a shallow CNN model with less than eight layers of convolutions [26], and thus, not considered for the current study. To capture the general behavioral pattern of CNN models across different sample frequency data was the main goal in this study, and it was assumed that the above mentioned four CNN model architectures would represent a broader CNN model family.

#### 2.3.1 Classical convolution-pooling network

Classical convolution-pooling represents a CNN model where a pooling layer always follows a convolution layer, forming a pair and in this study, two such convolution-pooling pairs were used followed by a classification block, which consists of a hidden dense layer followed by an output layer of two neurons for the QRS or non-QRS decision (Figure 3-a).

#### 2.3.2 Dense network, DenseNet

The Dense network model (DenseNet) is a densely connected convolutional network which connects each layer to every other layer in a feed-forward fashion [22] and consists of stacked dense blocks and transition layers. Dense blocks may contain several densely connected convolution layers, whereas, the transition layer down-samples its input dimension by employing a bottle-neck and a pooling layer. In this study a single dense block and a transition layer were used, where the dense block consisted of five densely connected convolution layers preserving the input resolution by applying proper padding (Figure 3-b). Finally, a classification block was used, similar to that of the classical convolution-pooling architecture (Figure 3-a), to get the final output.

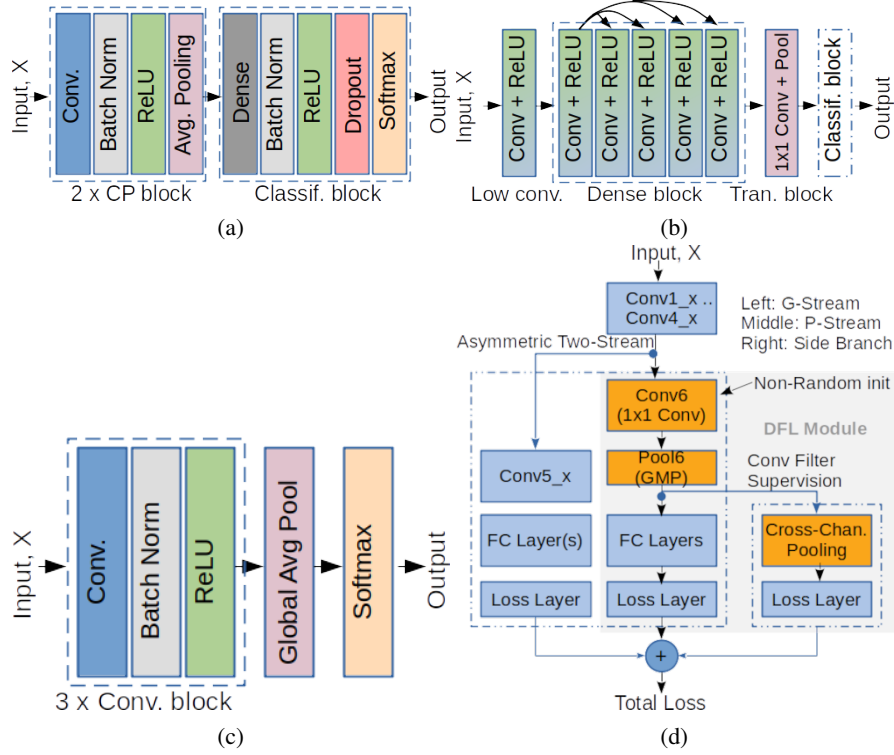


Figure 3: Four CNN models used in this study, (a) Classical convolution-pooling network (b) densely connected network (DenseNet), (c) Fully Convolutional network, and (d) discriminative Filter-bank learning (DFL). Note that the Classical conv-pooling network (Figure 3-a) consists of two sets of convolution-pooling (CP) pair, followed by a classification block, which consists of a hidden dense layer and the final softmax layer. The DenseNet (Figure 3-b) consists of a single densely connected block (of five convolution layers with proper padding to maintain the input and output resolution the same) and a transition-block (bottle-neck layer, followed by a pooling layer), followed by the same classification block of the Classical convolution-pooling network (Figure 3-a). The Fully convolutional network (Figure 3-c) consists of three convolution layers (convolution + batch-normalisation + activation) with proper padding (to maintain the input and output size constant), followed by a global-average-pooling and softmax layer. The DFL [21] is an approach to enhance the mid-level representation learning within the CNN framework, by learning a bank of convolutional filters (Figure 3-d). This consists of a global-stream (G-stream at the left branch, five Convolution layers, followed by a Dense and loss layer), discriminative patch stream (P-stream, 1x1 convolution followed by a global-max-pooling, Dense, and loss layer), and finally, a righthand side branch of cross-channel pooling (followed by a loss layer) for convolutional filter supervision and finally, all these losses combine to produce the final loss.

### 2.3.3 Fully convolutional network, FCN

The Fully convolutional network (FCN) was originally used for semantic segmentation of images [19], and later applied for time series classification [20] where a sequence of convolution layers were used and fully-connected layers were replaced by a global average pooling (GAP) layer. A similar approach was applied in this study where three convolutional blocks (i.e. a convolution block = convolution layer + batch normalisation + activation layer) were followed by a global-average-pooling (GAP) layer and finally a traditional softmax classifier was fully connected to the GAP layer’s output (Figure 3c).

### 2.3.4 Discriminative filter-bank learning, DFL

A discriminative filter bank within a single convolutional network context can be trained for fine-grained recognition [21] in image data and found promising (Figure 3-d). In this approach, the low-level convolution features are passed through two asymmetric streams - global feature learning stream (G-stream) and discriminative patch learning stream (P-stream) and additionally, forking a side branch from the global-max-pooling (GMP) output of the P-stream and passing through a cross-channel pooling for convolutional filter supervision. As shown in the Figure 3-d, the 1x1 convolutional layer in the P-stream may not trigger at the discriminative patches, however, to do that a direct supervision

was imposed at the 1x1 filters by introducing a cross-channel pooling layer followed by a softmax loss layer. A one-dimensional counterpart of the approach was implemented for QRS detection task, in this study.

## 2.4 Model hyper-parameters

Model hyper-parameters generally require optimization to find the best working model for a particular dataset. The focus of this study is to observe the effect of sampling frequency on the CNN model generalisation, instead of finding the best model. Model hyper-parameters were chosen for a particular model keeping the number of trainable parameters as low as possible and at the same time, maintaining higher accuracy levels. Each of the four models went through such optimisations as described below and the selected models configurations are summarised in the Table 1.

Table 1: Configuration information of the four CNN models (Classical convolution-pooling, Fully convolutional network, Discriminative filter-bank learning, and DenseNet) used in this study.

<i>Model</i>	<i>Config name</i>	<i>Config value</i>
Classical CNN	Conv-pooling pair	2
	Conv in, out-channel	1, 5
	Average pooling	/2
	Hidden dense neurons	50
FCN	Convolution blocks	3
	Conv channels per block	128, 128, 2
DFL	No. of init conv layers	4
	Streams after low-conv	2 (g/p-stream)
	Init. conv out-channel	64
	G-stream conv out-channel	16
	P-stream conv out-channel	64
DenseNet	No. of dense blocks	1
	No. of transition layer	1
	No. of conv-layers in dense block	5
	Dense block conv out-channels	32
	Tran. layer conv out-channels	32
	Tran. layer avg pooling	/2
	Hidden dense neurons	half of the flattened feat.
* All models	Conv kernel size	44 ms equiv.

### 2.4.1 Classical convolution-pooling model parameters

Classical CNN model generally consists of multiple pairs of alternate convolution-pooling layers where the use of a single convolution-pooling pair is the minimum. Two pairs of convolution-pooling blocks were found better compared to the minimum configuration of a single pair-block and so, was used for this study. The number of convolution output channels was set to five, since choosing a higher number of channels did not produce remarkable improvement. A pooling of stride two was chosen considering two facts - (i) greater number of strides leads to insufficient number of features available in 50Hz sample frequency data for two pairs of convolution-pooling blocks, and (ii) higher number of strides may lead to information loss in time series data.

### 2.4.2 Fully convolutional network parameters

FCN employs multiple convolution blocks (one conv block = convolution + batch-normalisation + activation) and the minimum configuration is to use a single such block. A model of three convolution blocks was found sufficient (i.e. no remarkable performance improvement with more convolution blocks), with the number of convolution output channels 128, 128, and 2. The number of output channels in the last convolution layer was set to two, due to the fact that the global-average-pooling (GAP) layers reduces each channel features to a single scalar, and in this way, two scalar outputs of the GAP layer goes into the final softmax layer for the binary classification.

### 2.4.3 Dense network parameters

DenseNet consists of a sequence of dense block and transition layer and the minimum configuration was found optimum for this study which consists of a single dense block of five convolution layers followed by a transition layer. Each convolution layer, in the dense-block, produces 32 feature-maps (number of convolution output channels), which is

concatenated, in the depth direction, to all the previous convolutions feature-maps. For example, the second convolution layers inputs 32 channel data (output of 1st convolution layer is 32), but the third convolution layer inputs 64 channel data (i.e.  $32 * 2 = 64$  for two previous convolution layers) and produces 32 channel output, and so on. The number of convolution output channels was set to 32 as a base value and further optimisation could be possible, however, no significant improvement was encountered using greater number of channels or greater number of dense block and transition layers. The transition layer performs a convolution using  $1 \times 1$  kernel to capture across-the-channel features and produces the same 32 channel output feature-maps, which then goes through an average pooling layer for sub-sampling. The number of output neurons in the hidden dense-layer was not fixed to a single value, rather, it was set dynamically as the half of the number of flattened features from the previous layer. This decision was made because with different number of flattened number of features (due to different sample frequency data), the same number of neurons (in the hidden dense layer) may not be proportionate across different input resolution data (due to different sampling frequency). For example, the number of neurons in the hidden dense layer of 200, may not be suitable for the flattened number of feature of 30 (i.e. for 50Hz data), but may seem fair enough for flattened number of feature of 400 (i.e., for 1000Hz data).

#### 2.4.4 Discriminative filter-bank learning model parameters

The DFL model architecture, at the end of the fourth convolution layer in the initial convolution block, outputs 64 channel feature-maps, which is then transformed into 16 channels in the G-stream convolution, and into the same 64 channels (but using  $1 \times 1$  convolution) in the P-stream convolution. After passing through a global-max-pooling, a cross-channel-pooling (in the side branch, right hand side in Figure 3-d) was performed by dividing 64 channels into two groups (due to binary classification) of 32 channels each. The number of channels in each group may be optimised to be as low as 16 (or 8), or as high as 64 (or 128), however, 32 channels produced a reasonable performance with moderate network complexity (more channels lead to more trainable parameters) and no significant performance improvement was observed using the mentioned variations.

#### 2.4.5 Common CNN hyper-parameters

The size of the convolution kernel was set for the initial convolution layer, following a similar strategy to [9], equivalent to 44 ms and this remains unchanged for all the convolution layers throughout all the CNN models. The average duration of the QRS complex is 60 ms, thus, 44 ms equivalent samples, as a convolution kernel, should be small enough to capture most ECG features. The convolution kernel size for 50Hz, 100Hz, 250Hz, 500Hz, 1000Hz and 2000Hz sampled data, thus, consist of 3, 5, 11, 23, 45 and 89 number of samples.

The number of epoches was fixed to ten for all the models at each sample frequency. It can be argued that different models may converge at different rates during the training process, which may require variable number of epoches. However, in this study, CNN models were treated equally to better compare their capabilities against a common set of parameters.

### 2.5 Model Testing

Both intra and inter-database testing were carried out in this study, following approaches similar to the study [8], where the intra-database tests reveal the subject-wise generalisability within the same database, and the inter-database tests explore a model's generalisation power across unknown validation databases with, possibly, different recording environment and patient-level data variance. The segmentation process yields more negative segments from each recording. To maintain the class balance, the policy of undersampling the majority class (negative segments) was adopted (negative labeled segments were randomly selected and removed from the training dataset). All the simulations were carried out in a multi-GPU server (with GeForce GTX 1080 Ti) sequentially in order to avoid any impact that may arise due to concurrency. Ideally, most of these simulations may be possible to run in a computer with limited resources, however, due to the loading of training and validation datasets (single training and two validation datasets per model per sampling frequency simulation) into memory may limit the execution of a comparatively complex model (DFL and DenseNet) simulation.

#### 2.5.1 Intra-database test

Intra-database testing was performed using subject-wise five-fold cross validation. Being subject-specific, the five-fold becomes unbiased, because the fraction of a validation record does not involve in the model training. A particular model performs such an intra-database testing for each of the six sampling frequency version of a dataset. For example, the classical convolution-pooling model performs five-fold cross validation on MIT-BIH arrhythmia dataset for six different target frequencies (MIT-BIH 50Hz, 100Hz, 250Hz, 500Hz, 1000Hz, and 2000Hz). The best model was the one that

persisted from the epoches for each fold of the five-fold operation (yielding five such best models) for later use with the cross-database validation, which is likely to enhance the cross-database validation scores.

### 2.5.2 Inter-database test

Inter-database or cross-database testing, on the other hand, was used to analyse the impact of the model’s generalisation capability on six different sample frequency variations of the datasets. Three datasets (MIT-BIH, INCART and QT) were used in this study where a model, which was trained using one particular dataset (say, MIT-BIH), gets a chance to be validated against the other two datasets (INCART and QT). Since six different sampling frequency versions of a dataset exists, so, in this study, a particular model (say, classical convolution-pooling) trained on six different sample frequency variations of a dataset (say, MIT-BIH 50Hz, 100Hz, 250Hz, 500Hz, 1000Hz, and 2000Hz) and then validated on the six corresponding sample frequency versions of other two datasets (INCART and QT 50Hz, 100Hz, 250Hz, 500Hz, 1000Hz, and 2000Hz). For a particular training database, sampled at one of the six frequencies, five different persisted best trained models (achieved during the five-fold intra-database validation process) were used to validate the other two validation datasets and finally, five such validation accuracy values (per validation database) were averaged to report final validation score for that validation database. In this way, it was expected to explore the relationship between the model’s generalisation capacity and the sampling frequency of the signal for the QRS detection task.

## 3 ECG Data

From the PhysioNet physiological and clinical data collection [5], three publicly available datasets (MIT-BIH arrhythmia, INCART, and QT) were used in this study. The MIT-BIH arrhythmia database is sampled at 360Hz and contains 48 half-hour two channel recordings. The INCART is a twelve-lead 75 recordings of 30 minutes length which is sampled at 257Hz, whereas, the QT consists of two-channel fifteen minutes recording of 105 subjects (usable only 82 recordings, as the annotation files available) sampled at 250Hz. This study used single lead data from the recordings of each dataset, where channel-1 data used from INCART and QT datasets, and for MIT-BIH, either modified-lead II or V1 lead data was used.

## 4 Results

### 4.1 Effect of sampling frequency on individual model generalisability

This study explores a CNN-based model’s generalisation capability using intra and inter-database validation. These validation results are presented under two views - (i) individual CNN-based model’s generalisability on different databases, and (ii) CNN-based models performance summarised across databases. The individual model’s generalisability is described below, whereas, the models’ summarised performances are presented in the following section.

#### 4.1.1 Intra-database performance

The results of the five-fold intra-database tests of four different CNN models operating on three datasets are represented in the Figure 4. MIT-BIH shows it’s superiority over the other two datasets in all the CNN models (classical convolution-pooling, FCN, DFL, and DenseNet), whereas, QT is the second best for two CNN models (classical convolution-pooling and FCN), and INCART is so for the other two models (DFL and DenseNet at 100Hz onwards). 250Hz is the turning point for two models (classical convolution-pooling and FCN) where INCART reaches it’s peak (Figure 4-a, b), whereas, 100Hz is the turning point for other two models for INCART reaching it’s peak and at the same time, surpasses QT (Figure 4-c, d).

#### 4.1.2 Inter-database performance

The Figure 5 shows frequency-wise inter-database validation accuracy of each CNN model (average of five cross-database validation scores, received during each fold of the five-fold intra-database validation, per frequency). The superiority of the INCART as a training dataset is visible which yields the maximum validation score for the MIT-BIH validation dataset for all the models, except for the classical convolution-pooling model where the QT as a training dataset achieves the maximum validation score for the MIT-BIH. At 50Hz, the validation scores are at the minimum levels, and the validation performance improvement beyond the 100Hz sampling frequency (sometimes 250Hz, for example, in classical convolution-pooling model the mit-validation-incart line) is marginal.



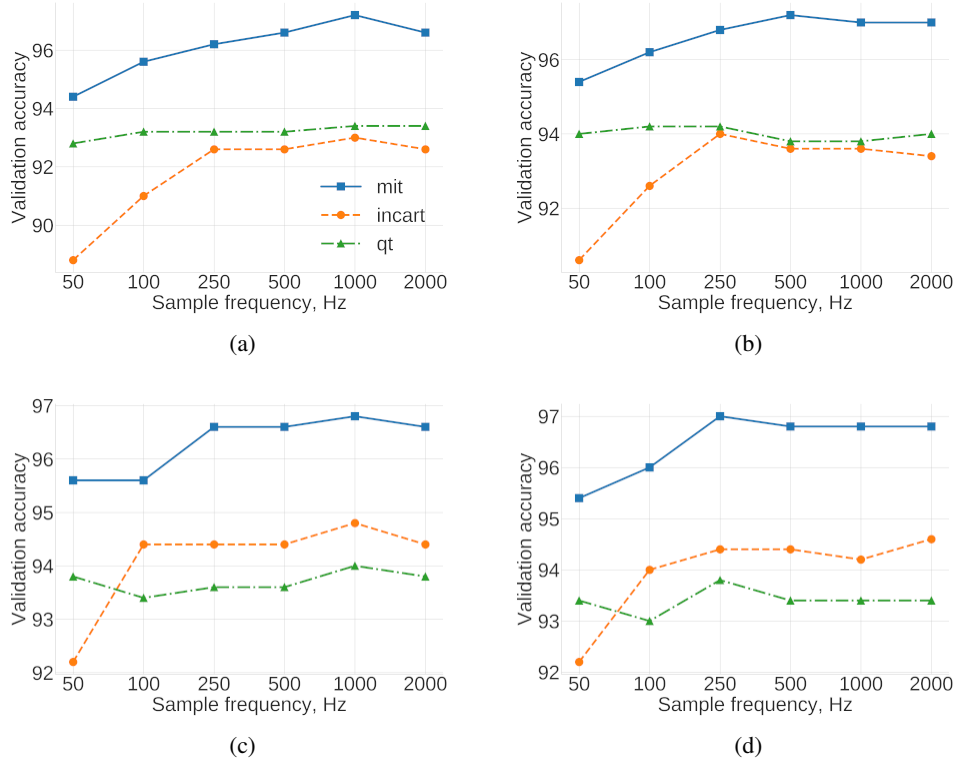


Figure 4: Frequency-wise intra-database test accuracy of different CNN models, namely, (a) classical convolution-pooling, (b) fully convolutional network (FCN), (c) discriminative filter-bank learning model (DFL), (d) dense network (DenseNet) for the QRS detection task. Subject-wise five-fold validation was performed on three ECG datasets (MIT-BIH, INCART, and QT).

## 4.2 Effect of sampling frequency on performance of CNN models

The performance of four CNN-based models were grouped together per sample frequency in order to observe comparative behavior clearly. In addition, database-wise variations were further summarised into a single value (i.e. median value) for the CNN-based models for different sample frequencies. These representations were performed for both intra and inter-database validations as below.

### 4.2.1 Intra-database performance

The results of intra-database testing, represented as the median interquartile-range box-plots in the Figure 6-a, are the five-fold average values of the three ECG datasets (MIT-BIH, INCART, and QT) which are grouped for each sampling frequency for the four different network architectures. There is an increasing trend of the accuracies, represented as the upper quartiles, from the lower to the higher sample frequencies for all the models, except for the case of 2000Hz, where it is slightly decreasing for two models (classical conv-pooling and DFL). The increase of accuracy from 50Hz to 100Hz is steeper compared to the increase from 100Hz to 250Hz, and the increase, for the higher frequencies (i.e. 500, 1000 and 2000Hz), is marginal (excepting the above mentioned two cases). In the classical conv-pooling model, for example, the peak accuracy increased 1.2% from 50Hz to 100Hz and half (i.e. 0.6%) from 100Hz to 250Hz, whereas successive increase rates are either marginal (i.e. 0.4% from 250-500Hz), equal (i.e. 0.6% from 500-1000Hz) or negative (i.e. -0.6% from 1000-2000Hz). The negative increase rate of -0.6% from 1000Hz to 2000Hz in the classical conv-pooling model follows the similar decreasing pattern for the DFL model (i.e. -0.2%), however, for the FCN and DenseNet, the increasing rate is 0% and 0.2% respectively. The interquartile range (represented as solid boxes in the figure) is smaller at 100Hz (for DenseNet and DFL) and at 250Hz (for alternate conv-pooling).

The median accuracy line (Figure 6-b) summarises (hiding database wise variations) the intra-database median behavioral response of each model on different sample frequencies. Classical convolution-pooling model rises to the peak at two steps, first at 100Hz and then at 1000Hz, with an increase of less than 0.25%. The DFL also follow the

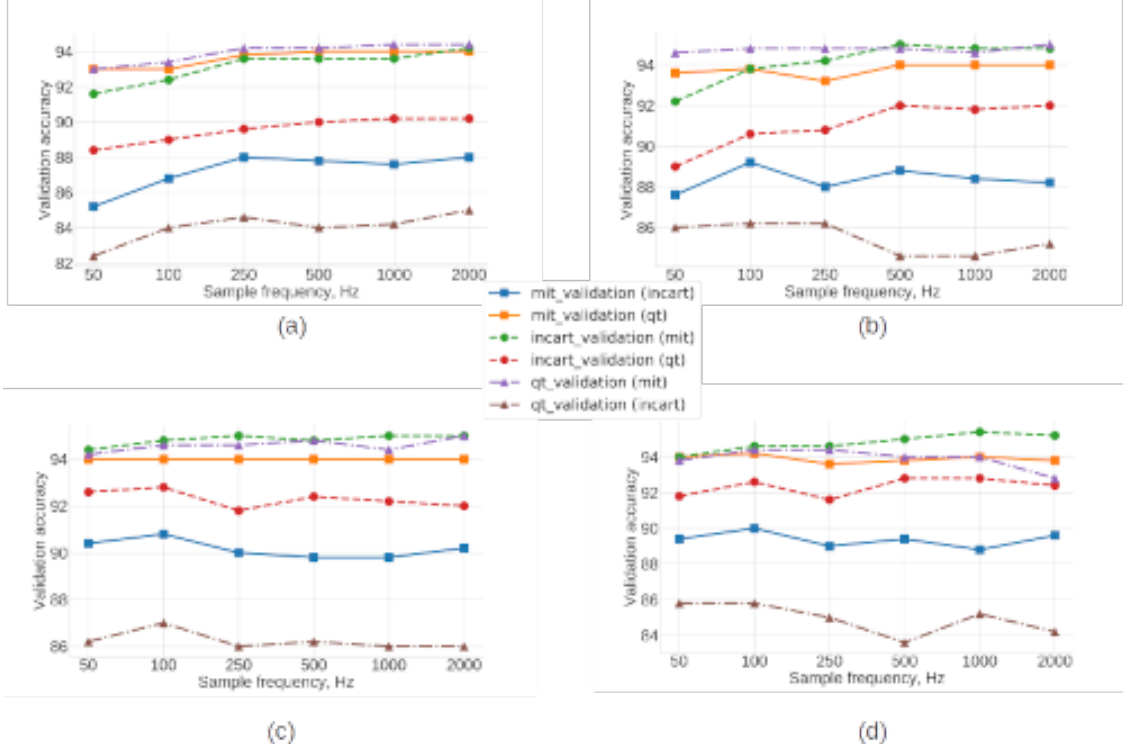


Figure 5: Frequency-wise cross-database validation accuracy of different CNN models, namely, (a) classical convolution-pooling, (b) fully convolutional network (FCN), (c) discriminative filter-bank learning model (DFL), (d) dense network (DenseNet). Three different ECG datasets (MIT-BIH, INCART, and QT) were used in testing, where a CNN model that is trained with a dataset, later used to validate against other two datasets. Pair of lines with similar line style (solid, dashed or dash-dotted) represents pair of validation datasets for a training dataset that can be found in the legend accordingly. For example, a solid line indicates a model trained with MIT-BIH dataset and the solid-blue, and solid-yellow lines indicate two validation datasets (INCART, and QT) accordingly. The best model was retrieved per fold (from the five-fold intra-database testing) and a cross-database validation was performed, yielding five cross-database validation scores which were then averaged.

same two-step rising pattern (at 100hz and 1000Hz) with an increase of less than 0.30%, as well as, the DenseNet that touches the peak at 250Hz and then at 2000Hz. The Fully Convolutional network shows its superiority at 250Hz, and the DenseNet, on the otherhand,

#### 4.2.2 Inter-database performance

The result, represented as the median interquartile-range box-plots in the Figure 7-a, summarizes the cross database accuracy of the models for different sampling frequencies. The upper quartiles of the interquartile range is the lowest at 50Hz for all the four models. The upper quartiles are at the highest levels at 100hz for DenseNet, at 500Hz for FCN, and at 2000Hz for the rest two models (classical conv-pooling and DFL). The interquartile range is shorter at 100Hz (classical convolution-pooling, FCN, and DFL), and at 2000Hz (DenseNet).

The median accuracy line (Figure 7-b) summarises (hiding database wise variations) the cross-database median behavioral response of each CNN model on different sample frequencies. At 100Hz, the DenseNet and DFL shows the highest cross-database accuracy, although, DenseNet is very close at two other frequencies (500 and 1000Hz) and drops afterwards. At 250Hz, the classical convolution-pooling hits the peak and then has a marginal increase with the increase in frequencies. The FCN hits the peaks at 100Hz and 500Hz, then shows a marginal increase from 1000Hz onwards, after a decreasing period starting from the 2nd peak.

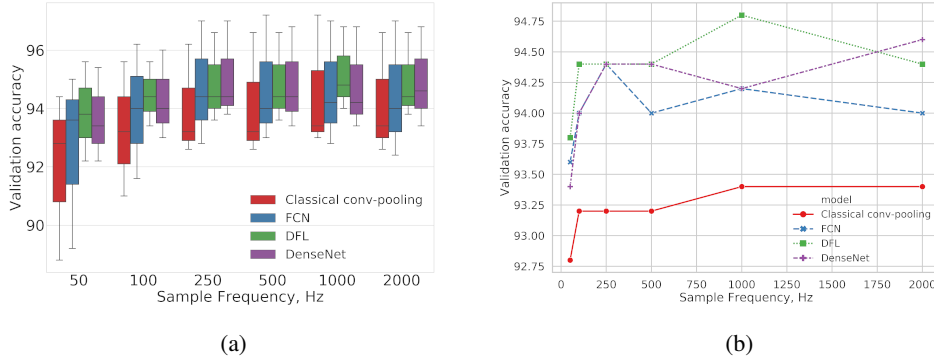


Figure 6: (a) Median interquartile-range box-plot represents sampling frequency-wise five-fold validation accuracy grouped by four different convolutional network (CNN) based-model architectures (classical conv-pooling, fully convolutional network, discriminative filter-bank learning, and dense-network) for QRS detection task, and (b) represents the median accuracy lines summarizing median effects (of three intra-database validation scores across three datasets) at each frequency. Record-wise five-fold validation accuracy values were taken from three datasets (MIT-BIH arrhythmia, INCART, and QT) per CNN model architecture per sampling frequency. For example, the red box at 50Hz represents quartiles of three K-fold validation accuracies (of MIT-BIH, INCART and QT datasets accordingly) for classical conv-pooling CNN architecture, where, the min, median and max values are 88.8%, 92.8%, and 94.4% respectively.

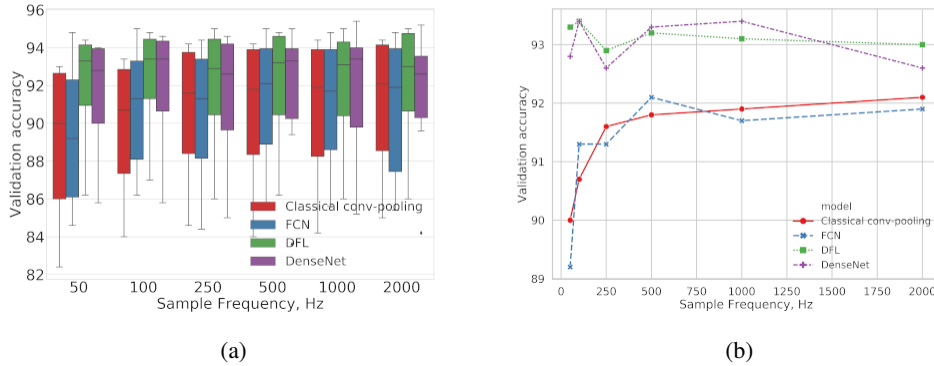


Figure 7: (a) Median interquartile-range box-plot represents sampling frequency-wise cross database validation accuracy grouped by four different CNN model architectures (i.e. classical conv-pooling, fully convolutional network, discriminative filter-bank learning, and dense-network) for QRS detection task, and (b) represents the median accuracy lines summarizing the median effects at each frequency (of six cross-database validation scores across three datasets). Cross database validation was obtained for three different databases (i.e. MIT-BIH arrhythmia, INCART, and QT), where, for each training database, other two databases are for validation. For each sampling frequency and CNN architecture, six such cross validation accuracies can be obtained. For example, the red box at 50Hz represents the quartiles of six validation accuracy values (i.e. two validation accuracy for each of the MIT-BIH, INCART, and QT respectively) for the classical conv-pooling architecture, where, the min, median and max values represent 82.4%, 90.0% and 93.0% respectively. The (b) part calculates the median of these six accuracy values per sample frequency.

### 4.3 Model costs

Deep learning models have costs which were observed in terms of the number of trainable parameters (Table 2 and Figure 8-a) and the training time (Figure 8-b).

#### 4.3.1 Trainable number of parameters

The Table 2 shows the number of trainable parameters of four different deep learning models operating on datasets sampled at six different frequencies and the Figure 8-a plots these values in  $\log_2$  scale. The alternate conv-pooling

Table 2: The number of trainable model parameters for different CNN models.

Hz	Classical Conv-Pool	FCN	DFL	DenseNet
50	872	1542	54440	64786
100	1432	2310	89832	177874
250	3362	4614	192808	832434
500	6222	9222	298930	3148882
1000	12132	17670	506638	12040994
2000	23952	34566	994238	47105218

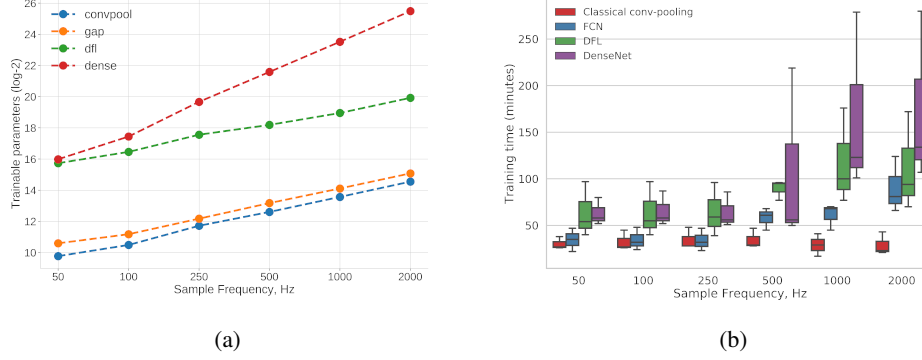


Figure 8: (a) The number of trainable model parameters for different CNN models (i.e. Alternate conv-pooling, FCN, DFL, and DenseNet) for each sampling frequency. The number of parameters vary due to the fact that the convolution filter size grows proportionately with the increase of the sampling frequency. Due to a large variation in the number of model parameters in different models, the y-axis values are taken in  $\log_2$  scale. Actual parameter numbers are mentioned in Table 2. (b) Median interquartile range box-plot represents sampling frequency-wise different CNN models training time combining three datasets (MIT-BIH, INCART, and QT). For example, at 50Hz sampling frequency, the training time of the DenseNet with three datasets are 49, 59, and 98 minutes, which are shown as the min, median and the max values in the blue box.

model has the lowest number of parameters to train at all the sample frequencies, which is relatively closely followed by FCN and distantly followed by DFL and DenseNet respectively.

#### 4.3.2 Training time

Figure 8-b represents the training time (in minutes) of the models (for three different datasets, summarised as a single colored box, representing an interquartile range) for different operating frequencies. As shown in the figure, there is a slowly increasing trend of the quartiles for all the CNN model architectures from 50Hz to 250Hz and a rapid increasing trend from 500Hz onwards (excepting the classical conv-pooling model which remains almost at the same level). There is an exponential increase of the training time from 250Hz to 500Hz to 1000Hz for the DFL and DenseNet. The FCN has a sharp increase in the training time from 250Hz to 500Hz and from 1000Hz to 2000Hz, whereas, it remains almost at the same level in the lower frequencies (50Hz, 100Hz, 250Hz, and 500Hz). The classical conv-pooling model shows almost similar levels of the upper quartiles for all the sampling frequencies.

## 5 Discussion

The findings of this study are discussed below.

### 5.1 Intra-database performance

The intra-database test results (Figure 4, and Figure 6) summarise the fact that different CNN models tend to gain increasing detection accuracies, but at a different rate, with an increase in the sampling frequency. The rate of increase is steeper from 50Hz through to 250Hz, compared to the higher frequencies, with each of the four CNN models showing almost similar patterns, although the magnitude of the accuracy increase changes at different proportions. Finer

resolution input data (higher sample frequency) seems not capable of increasing the model generalisation proportionately, which could be due to the fact that by taking an increasing number of samples of the QRS complex and non-QRS regions, marginal or no information gain may be achieved (as shown in the Figure 1). The lower accuracy levels at as low as 50Hz, on the other hand, indicates that information, at some extent, has been lost due to the lower sampling rate that keeps the CNN models from achieving the highest accuracy levels at these lower frequencies. One particular case is the QT database, for which, the accuracy at 50Hz is competitive to the other frequencies, which indicates that very little or no information gain is taking place with an increase in the sampling frequency, for that case.

## 5.2 Cross-database performance

The cross-database validation datasets, for each training dataset, of all the CNN models, maintains one kind of ordering (as shown in the Figure 5, qt-validation INCART line having the lowest and qt-validation MIT-BIH line with the highest accuracy values). Each model may have superiority over the others which is realised by observing the shifting of the validation accuracy lines at different magnitude across different frequencies, keeping this ordering unchanged. The consistent relative orderings of six different cross-database validation lines across different CNN models may be due to the fact that it is the very nature of the data itself which limits the maximum generalisability of a CNN model (irrespective of CNN architectures), keeping all other factors unchanged. Possibly, the uniqueness of the validation datasets (i.e., subject variance and signal noise) were not present in the training dataset to allow a CNN model to exceed this generalisability limitation, and this similar observation was discussed in a study [8], where it was concluded that the generalisation capability does not increase by simply adding more training samples, rather a diverse range of recordings should be included incorporating as much relevant patterns as possible. Another study [9] reiterates this fact stating that inclusion of as much heterogeneities as possible into the training data, possibly may increase a model's generalisation ability.

## 5.3 Performance of CNN models

Interestingly, the cross-database validation accuracy at, as low as, 100Hz is the maximum for two CNN models (DFL and DenseNet), and at 250Hz and 500Hz for the classical convolution-pooling and FCN respectively (Figure 7-b). The variation of the cross-database validation accuracies (Figure 7-a) summarizes that the lowest accuracy variation (low interquartile range) is observed at as low as 50Hz and 100Hz (for DFL model), although the upper quartile is the highest at higher frequencies (i.e. at 2000Hz with DenseNet). Also, this variation, at worst case, is less than 2% (for FCN, in Figure 7-b). CNN models, thus, may be capable of offering stable generalisation at lower frequency signals (i.e. 50, 100, or 250Hz), whereas, the data with the higher frequency introduces more variation. This phenomena may be justified by the fact that the lower frequency sampled data represents the detection artifacts (i.e. a QRS complex) with the minimum input resolution, yielding a lesser noise attenuation, whereas, the higher frequency data may introduce a significant proportion of noise (keeping the basic artifact morphology similar) that might lead to inconsistent generalisation for some of the CNN models. Another instance supports this phenomena, for example, the only CNN model that shows consistent intra-database performance improvement in higher frequencies (i.e. DenseNet at 1000Hz onwards, in Figure 6-b), shows an opposite behaviour in the cross-database validation, where it consistently decreases with an increase in the sample frequency (in Figure 7-b). Figure 1 probably justifies this phenomena which shows that the higher frequency introduces much fluctuation to the data as compared to the lower sample frequencies. The figure also justifies the fact that the lower frequency may significantly distort the morphology of the signal artifacts (the third beat as shown in the Figure 1-a) which may lead to poor detection performance and thus poor generalisation capability of CNN models.

## 5.4 Model cost and performance

With the increase of sampling frequency, CNN models input resolution and convolution filter size changes, yielding an exponentially increasing number of trainable model parameters (model complexity, in Figure 8-a). Training a CNN model with an increasing number of parameters may require an increasing number of training samples and computation resources. It is also clear that (as shown in the Figure 8-b) the CNN models with higher number of trainable parameters (yielding from higher sample frequency data) require comparatively higher training time. The variation of training time around 100Hz and 250Hz is negligible, however, for some models (DFL and DenseNet), it grows exponentially at 500Hz and 1000Hz. The negligible increase of the training time in lower sample frequency simulation may be justified by the fact that for a dedicated GPU of 10 giga-byte memory, the simulations of 50, 100 and 250Hz data failed to fully occupy the allocated computation resource compared to higher frequency simulations (500Hz onwards). The computed training time would have been different for the lower frequency data simulations (as well as the higher counterpart), if they were executed in a computer without a GPU.

## 5.5 Implications

Different application settings may require different detection accuracy levels and computation resources. For example, the QRS detection in wearables may prefer a light-weight solution where sacrificing 1% accuracy may not have a severe impact and can go for data sampled at as low as 50Hz, compared to the deployment in the clinical settings (e.g., in an intensive care unit), where a higher detection rate may be critical, thus, adoption of ECG data sampled at higher frequencies may be preferable, which is trained with a better generalising model (e.g. DenseNet or other).

Finally, the findings of this CNN-based QRS detection study can be summarised as below:

- Sample frequency as low as 50Hz, 100Hz or 250Hz yields an acceptable level of accuracy (while 50Hz shows comparatively the lowest performance at a margin around 2%)
- Higher sample frequencies contribute marginally to the accuracy gain (introducing more variations), however, such marginal increase may require a CNN model with a higher number of trainable parameters and higher training time.
- Some CNN model architectures show greater generalisability (i.e. DenseNet or DFL) compared to others (i.e. classical convolution-pooling or FCN).

## 6 Conclusion and Future Work

Detection of the QRS complex is necessary for automated ECG signal analysis and with the increasing usage of wearables in the home-based personal health monitoring, a careful selection of the data sampling frequency may be necessary in order to obtain a simpler deep learning based model. In this experimental research, the effects of data sampling frequency were investigated using three datasets (MIT-BIH, INCART, and QT) resampled at six different sample frequencies (50, 100, 250, 500, 1000, and 2000Hz) following both intra and inter-database testing methods. Four different CNN-based models (classical convolution-pooling, fully convolutional network, discriminative filter-bank learning, and dense network) were used to justify the findings. The results show that the model accuracy has a positive relationship with the sample frequencies across all the models at a varying magnitude. Data signal sampled at as low as 50Hz seems capable of representing ECG signal morphologies (the QRS complex), losing information (as well as detection accuracy) at a certain level, keeping the CNN model simple, as compared to the higher frequency counterparts, where increased signal resolution may not add much information proportionately. In addition, the higher frequency signals may have a chance of getting distorted due to the resampling method (i.e. interpolation). Lower resolution signals also show greater generalisability of the CNN model (i.e. at 100Hz or 250Hz), compared to the higher resolution signals (i.e. 2000Hz). The QRS detection accuracy variation is in the range of 2-3% from 100Hz to the higher frequency levels, however, the increase of the model complexity is much higher in the higher frequencies. To carefully design a training dataset which consists of enough heterogeneities for a suitable CNN-based model to have better generalisability could be one of the future tasks.

## References

- [1] Bert Uwe Köhler, Carsten Hennig, and Reinhold Orglmeister. The principles of software QRS detection. *IEEE Engineering in Medicine and Biology Magazine*, 2002. ISBN: 0739-5175 VO - 21.
- [2] Nagarajan Ganapathy, Ramakrishnan Swaminathan, and Thomas Deserno. Deep Learning on 1-D Biosignals: a Taxonomy-based Survey. *Yearbook of Medical Informatics*, 27(01):098–109, August 2018.
- [3] Mohamed Elgendi, Björn Eskofier, Socrates Dokos, and Derek Abbott. Revisiting QRS detection methodologies for portable, wearable, battery-operated, and wireless ECG systems. *PLoS ONE*, 2014. ISBN: 1932-6203.
- [4] Qingxue Zhang, Dian Zhou, and Xuan Zeng. HeartID: A Multiresolution Convolutional Neural Network for ECG-Based Biometric Human Identification in Smart Health Applications. *IEEE Access*, 2017. ISBN: 0902-4441; 0902-4441.
- [5] Ary L. Goldberger, Luis A. N. Amaral, Leon Glass, Jeffrey M. Hausdorff, Plamen Ch. Ivanov, Roger G. Mark, Joseph E. Mietus, George B. Moody, Chung-Kang Peng, and H. Eugene Stanley. PhysioBank, PhysioToolkit, and PhysioNet: Components of a New Research Resource for Complex Physiologic Signals. *Circulation*, 101(23), June 2000.
- [6] P. Laguna, R.G. Mark, A. Goldberg, and G.B. Moody. A database for evaluation of algorithms for measurement of QT and other waveform intervals in the ECG. In *Computers in Cardiology 1997*, pages 673–676, Lund, Sweden, 1997. IEEE.

- [7] Philip De Chazal, Maria O'Dwyer, and Richard B. Reilly. Automatic classification of heartbeats using ECG morphology and heartbeat interval features. *IEEE Transactions on Biomedical Engineering*, 2004.
- [8] Ahsan Habib, Chandan Karmakar, and John Yearwood. Impact of ECG Dataset Diversity on Generalization of CNN Model for Detecting QRS Complex. *IEEE Access*, 7:93275–93285, 2019.
- [9] Li Guo, Gavin Sim, and Bogdan Matuszewski. Inter-patient ECG classification with convolutional and recurrent neural networks. *Biocybernetics and Biomedical Engineering*, 39(3):868–879, July 2019.
- [10] Yozaburo Nakai, Shintaro Izumi, Masanao Nakano, Ken Yamashita, Takahide Fujii, Hiroshi Kawaguchi, and Masahiko Yoshimoto. Noise tolerant QRS detection using template matching with short-term autocorrelation. In *2014 36th Annual International Conference of the IEEE Engineering in Medicine and Biology Society*, pages 34–37, Chicago, IL, August 2014. IEEE.
- [11] Patrick S. Hamilton and Willis J. Tompkins. Quantitative Investigation of QRS Detection Rules Using the MIT/BIH Arrhythmia Database. *IEEE Trans. Biomed. Eng.*, BME-33(12):1157–1165, December 1986.
- [12] B. S. Chandra, C. S. Sastry, and S. Jana. Robust Heartbeat Detection From Multimodal Data via CNN-Based Generalizable Information Fusion. *IEEE Trans. Biomed. Eng.*, 66(3):710–717, March 2019.
- [13] Era Ajdaraga and Marjan Gusev. Analysis of sampling frequency and resolution in ECG signals. In *2017 25th Telecommunication Forum (TELFOR)*, pages 1–4, Belgrade, November 2017. IEEE.
- [14] Tjalf Ziemssen, Julia Gasch, and Heinz Ruediger. Influence of ECG Sampling Frequency on Spectral Analysis of RR Intervals and Baroreflex Sensitivity Using the EUROBAVAR Data set. *J Clin Monit Comput*, 22(2):159–168, April 2008.
- [15] Shadi Mahdiani, Vala Jeyhani, Mikko Peltokangas, and Antti Vehkaoja. Is 50 Hz high enough ECG sampling frequency for accurate HRV analysis? In *2015 37th Annual International Conference of the IEEE Engineering in Medicine and Biology Society (EMBC)*, pages 5948–5951, Milan, August 2015. IEEE.
- [16] P. Hamilton. Open source ECG analysis. In *Computers in Cardiology*, pages 101–104, Memphis, TN, USA, 2002. IEEE.
- [17] Yann LeCun, Yoshua Bengio, and Geoffrey Hinton. Deep learning. *Nature*, 521(7553):436–444, May 2015.
- [18] Kartik Audhkhasi, Osonde Osoba, and Bart Kosko. Noise-enhanced convolutional neural networks. *Neural Networks*, 78:15–23, June 2016.
- [19] Jonathan Long, Evan Shelhamer, and Trevor Darrell. Fully Convolutional Networks for Semantic Segmentation. In *Proceedings of the IEEE conference on computer vision and pattern recognition*, pages 3431–3440, 2015.
- [20] Zhiguang Wang, Weizhong Yan, and Tim Oates. Time series classification from scratch with deep neural networks: A strong baseline. In *2017 International Joint Conference on Neural Networks (IJCNN)*, pages 1578–1585, Anchorage, AK, USA, May 2017. IEEE.
- [21] Yaming Wang, Vlad I. Morariu, and Larry S. Davis. Learning a Discriminative Filter Bank Within a CNN for Fine-Grained Recognition. In *2018 IEEE/CVF Conference on Computer Vision and Pattern Recognition*, pages 4148–4157, Salt Lake City, UT, USA, June 2018. IEEE.
- [22] Gao Huang, Zhuang Liu, Laurens van der Maaten, and Kilian Q. Weinberger. Densely Connected Convolutional Networks. In *2017 IEEE Conference on Computer Vision and Pattern Recognition (CVPR)*, pages 2261–2269, Honolulu, HI, July 2017. IEEE.
- [23] John G Proakis and Dimitris G Manolakis. *Digital signal processing*. PHI publication, 2004.
- [24] AAMI ECAR. Recommended practice for testing and reporting performance results of ventricular arrhythmia detection algorithms. *Association for the Advancement of Medical Instrumentation*, page 69, 1987.
- [25] Kaiming He, Xiangyu Zhang, Shaoqing Ren, and Jian Sun. Deep Residual Learning for Image Recognition. In *2016 IEEE Conference on Computer Vision and Pattern Recognition (CVPR)*, pages 770–778, Las Vegas, NV, USA, June 2016. IEEE.
- [26] Awni Y. Hannun, Pranav Rajpurkar, Masoumeh Haghpanahi, Geoffrey H. Tison, Codie Bourn, Mintu P. Turakhia, and Andrew Y. Ng. Cardiologist-level arrhythmia detection and classification in ambulatory electrocardiograms using a deep neural network. *Nat Med*, 25(1):65–69, January 2019.